

HIGH PRESSURE METAMORPHIC CONDITIONS IN GARNET AMPHIBOLITE FROM A COLLISIONAL SHEAR ZONE RELATED TO THE TAPO ULTRAMAFIC BODY, EASTERN CORDILLERA OF CENTRAL PERU

Arne P. Willner⁽¹⁾, Ricardo Castroviejo⁽²⁾, José F. Rodrigues⁽³⁾, Jorge Acosta⁽⁴⁾, Miguel Rivera⁽⁵⁾

⁽¹⁾ Institut für Geologie, Mineralogie und Geophysik, Ruhr-Universität, 44780 Bochum, Germany, arne.willner@rub.de; ⁽²⁾ Universidad Politécnica de Madrid, ETSI Minas, c/ Ríos Rosas, 21, 28003_Madrid, ricardo.castroviejo@upm.es; ⁽³⁾ Fac. Engenharia Univ. Porto (FEUP), r. Dr. Roberto Frias s/n 4200-465 Porto, Portugal, felic@fe.up.pt; ⁽⁴⁾ INGEMMET, Dirección de Recursos Minerales y Energéticos, Av. Canadá 1470. Lima 41- Perú. jacosta@ingemmet.gob.pe; ⁽⁵⁾ Miguel Rivera Feijóo, Av. Dos de Mayo 1312-503, Lima 27; mrivera@mineral-r.com.

INTRODUCTION AND SETTING

A discontinuous belt of elongated ultramafic rock bodies (mostly serpentinites) occurs in the Eastern Cordillera of the central Peruvian Andes. One of the main occurrences is the Tapo Massif, a lense-shaped serpentinite body, ~2 km x 5 km, comprising small podiform chromitite deposits (Castroviejo et al., 2009) and bands or lenses of garnet-amphibolite, both strongly sheared and thrust upon the upper Paleozoic sediments of the Ambo Group (Fig. 1). Metabasite geochemistry suggests a mid-ocean ridge or an ocean island protolith. The whole sequence can be interpreted as a disrupted ophiolitic complex (Castroviejo et al., 2010). The geological setting of the Tapo occurrence is described by J.F. Rodrigues et al. (2010). To get information about its geotectonic setting we applied new geothermobarometric techniques to the garnet amphibolite. Finding representative samples with an adequate mineralogy to apply these techniques is in this case a difficult task. A common problem is the almost ubiquitous overprinting by serpentinisation or retrograde metamorphism and, locally, by metasomatism or alteration enhanced by deformation, producing a variety of rock types, as rodingites, birbirites and listvaenites. Nevertheless, careful sampling followed by petrographic examination of the rocks allowed to identify some samples in which useful assemblages are present.

ASSEMBLAGES AND MINERAL CHEMISTRY

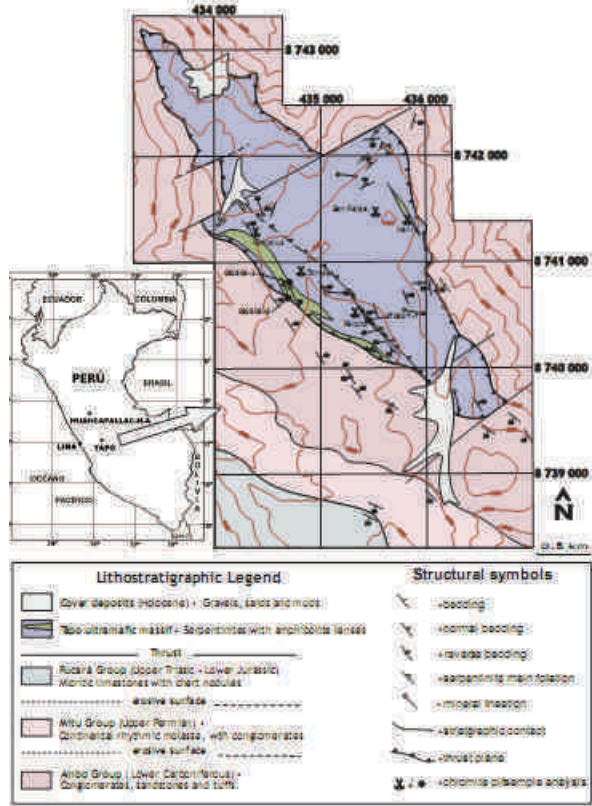
We selected three garnet amphibolite samples¹ (090606-2, 090606-3 and 270607-7, Fig. 1) which contain the assemblage garnet-Ca-amphibole-epidote-chlorite-albite-quartz-titanite-ilmenite. Additionally clinopyroxene is present in sample 090606-3. This assemblage points to conditions of the albite-epidote amphibolite facies.

Garnet is essentially an almandine-grossular solid solution (almandine_{0.46-0.62}grossular_{0.25-0.45}pyrope_{0.01-0.18}spessartite_{0.02-0.11}). Almandine and pyrope contents increase from core to rim, whereas spessartite decreases and grossular contents show little variations. Amphibole compositions vary strongly between samples: in sample 090606-3 amphibole is actinolite to magnesiohornblende (Na 0.10-0.66 apfu, Na_A 0.0-0.66 apfu, X_{Mg} 0.42-0.68), in sample 270607-7 magnesiohornblende to tschermakite (Na 0.58-1.03 apfu, Na_A 0.36-0.82 apfu, X_{Mg} 0.25-0.46) and in sample 090606-2 tschermakitic hornblende to tschermakite (Na 0.05-0.80 apfu, Na_A 0.3-0.5 apfu, X_{Mg} 0.41-0.58). Epidote composition within all samples varies strongly (X_{pistacite}=0.4-0.9) contrasting that of chlorite (Si 5.3-5.7 apfu; X_{Mg} 0.35-0.51). Clinopyroxene composition is diopside_{0.56-0.58} hedenbergite_{0.20-0.30} acmite_{0.07-0.10} orthopyroxene_{0.02-0.05} tschermak component_{0.02-0.07}. Plagioclase is invariably albite.

GEOTHERMOBAROMETRY

We calculated pseudosections for the three metabasite samples using the PERPLE_X software package (Connolly 2005). The thermodynamic data set of Holland & Powell (1998, updated 2002) for minerals and aqueous fluid was used. Calculations were performed using the following solid-solution models: for epidote, garnet, plagioclase, clinopyroxene, omphacite, amphibole and chlorite by Holland

& Powell (2003) and Powell & Holland (1999). For the calculation of the pseudosections the major element compositions analysed by XRF were simplified to a 9-component system ($\text{SiO}_2\text{-TiO}_2\text{-Al}_2\text{O}_3\text{-FeO-MgO-CaO-Na}_2\text{O-H}_2\text{O-O}_2$) normalized to 100% (Table 1). Water contents were augmented to excess water conditions that are considered to have prevailed during peak PT-conditions. Oxygen contents were arbitrarily chosen to account for epidote and Fe^{3+} -rich clinopyroxene present in the samples. Calculated compositions of minerals provide good coincidence with measured ones (Table 2) except partly for amphibole, because solid solution models for amphibole are still not optimal.



restricted for sample 090606-2 at 12-13 kbar, 530-540°C. Chlorite, albite and ilmenite are considered as retrograde phases in sample 090606-3, as albite, quartz and titanite in sample 270607-7 and albite in sample 090606-2.

Fig.2 Stability fields of minerals deduced from PT-pseudosections calculated from whole rock compositions (Table 1) in the system $\text{SiO}_2\text{-TiO}_2\text{-Al}_2\text{O}_3\text{-FeO-MgO-CaO-Na}_2\text{O-H}_2\text{O-O}_2$. Grey fields represent the stability field of the assemblages in the respective samples which represent peak PT-conditions. Abbreviations: Ab-albite, Am-Ca-amphibole, Chl-chlorite, Cpx-clinopyroxene, Ep-epidote, Gt-garnet, Im-ilmenite, Lw-lawsonite, Mt-magnetite, Pl-plagioclase, Rt-rutile, Tt-titanite.

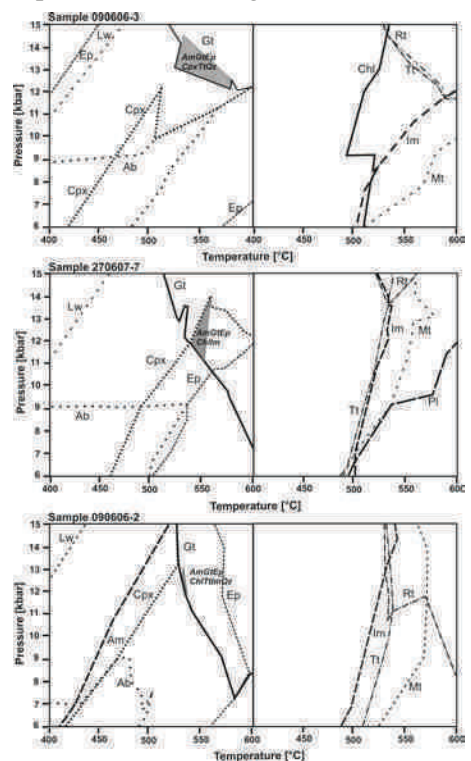
Fig.1. Geological map of the Tapo Ultramafic Complex with indications of the sample localities.

We simplified the pseudosections to present mere stability fields in the PT-range 400-600°C, 6-15 kbar in Fig.2. Garnet appears in the metabasite at conditions exceeding 8 kbar and 520°C. Whereas chlorite, epidote and Ca-amphibole are mostly stable in the considered PT-range, titanite is replaced at temperatures >520°C by ilmenite or rutile (>10 kbar). Albite is stable up to 520°C, 9 kbar and is partly replaced by plagioclase at higher temperature. Fe^{3+} -rich clinopyroxene is stable up to about 7 kbar, 450°C and 12 kbar, 550°C, whereas omphacite was not formed under the considered conditions and compositions according to our calculation.

The assemblages representing peak metamorphic conditions coincide for all three selected samples within a range of 525-575°C,

11-14

kbar,
more



CONCLUSIONS

We can restrict the peak metamorphic conditions for the Tapo Ultramafic Complex to 12.5 ± 1 kbar and $535 \pm 20^\circ\text{C}$ corresponding to 41-48 km burial depth (calculating with a mean crustal density of 2.8 g/ccm) and a low metamorphic geotherm of $10-13^\circ\text{C}/\text{km}$. Such conditions occur in subduction settings and collisional belts. Similar conditions were derived e.g. by Massonne & Calderón (2008) in a Devonian collision zone between an exotic microplate ("Chilenia") and the South America. A comparable situation might also be conceivable for the situation in the Eastern Cordillera of Peru.

REFERENCES

- Castroviejo R et al. (2009) Proc. *10th. Biennial SGA Meeting*, Townsville, Australia: 927-929.
 Castroviejo R et al. (2010) *Ophiolites in the Eastern Cordillera of the central peruvian Andes. IMA2010: 20th General Meeting of the International Mineralogical Association* (in press)
 Connolly JAD (2005) *Earth and Planetary Science Letters* 236: 524-541.
 Holland TJB, Powell R (1998) *Journal of Metamorphic Geology* 16: 309-343.
 Holland TJB, Powell R (2003) *Contributions to Mineralogy and Petrology* 145: 492-501.
 Massonne HJ, Calderón M (2008) *Revista Geologica de Chile* 35: 215-231.
 Powell R, Holland TJB (1999) *American Mineralogist* 84, 1-14
 Rodrigues JF et al. (2010) *Geología y Estructura de las Ultramafitas de Tapo y Acobamba (Tarma, Perú). Removilización tectónica andina de un segmento ofiolítico pre-andino.* (This vol.)

TABLE 1

(a) Whole rock compositions of metabasite			(b) Simplified compositions used for calculations of the pseudosections		
090606-	090606	270607	090606	090606	270607-
(wt-%)	3	-2	-7	(wt-%)	7
SiO₂	49,43	40,01	40,35	SiO₂	47,28
Al₂O₃	11,55	10,11	10,99	Al₂O₃	11,05
Fe₂O₃	14,13	21,86	23,35	FeO	12,18
MnO	0,15	0,18	0,25	MnO	0,14
CaO	10,84	8,11	8,88	CaO	10,37
MgO	6,80	7,96	6,82	MgO	6,50
Na₂O	3,06	0,22	1,97	Na₂O	2,93
K₂O	0,12	0,06	0,12	TiO₂	2,46
TiO₂	2,57	3,26	5,09	H₂O	7,00
P₂O₅	0,13	0,01	<0,050	O₂	0,10
LOI	1,03	8,03	2,18	Sum	100,00
Sum	99,81	99,81	99,99		100,00

Table 2. Representative mineral analyses and mineral compositions calculated with PERPLE_X for comparison.

Line	090606	090606	090606	090606	090606	090606	090606	090606	090606	090606	090606	090606	090606	090606	090606	090606	090606	
	-3	-3	Game	-3c	-3f	-3	-2f	-2	-2c	-2f	-2	-2c	-2f	-2	-2c	-2f	-2	
NiO	0.30	0.30	W102	34.34	34.73	0.30	38.20	0.30	34.44	34.14	0.30	30.01	40.40	0.30	44.29	0.30	32.70	0.30
Al2O3	1.43	1.43	C/Al2O3	21.04	21.04	133 C/	21.73	133 C/	21.07	21.11	140 C/	Al2O3	14.13	14.13	9.77	133 C/	1.43	133 C/
TiO2	0.17	0.17	TiO2	0.17	0.17	0.17	0.04	0.17	0.17	0.17	0.17	TiO2	0.13	0.13	0.15	0.17	0.07	13.17
Fe2O3	3.74	3.74	Fe2O3	0.78	0.78	0.78	0.00	0.78	0.78	0.78	0.78	Fe2O3	4.94	4.94	4.47	3.71	3.71	3.71
FeO	7.14	7.14	FeO	21.26	21.42	7.14	22.81	7.14	22.42	22.34	7.14	FeO	20.14	20.14	11.99	12.77	7.14	7.14
MnO	0.09	0.09	MnO	4.39	0.94	0.09	0.30	4.39	3.27	MnO	4.49	MnO	4.49	0.79	13.72	0.09	0.09	
MgO	11.38	11.38	MgO	0.32	1.13	0.32	0.47	0.32	0.32	0.32	MgO	10.79	MgO	10.79	10.34	11.77	0.32	0.32
CaO	24.14	24.14	CaO	14.23	14.16	24.14	1.11	14.23	11.11	14.23	CaO	0.00	CaO	0.00	0.01	0.02	0.02	0.02
H2O	0.14	0.14	H2O	96.18	96.18	0.14	100.00	96.18	99.46	99.70	H2O	0.11	H2O	0.11	0.07	0.07	0.07	0.07
SuM	99.74	99.74	SuM	2.1	2.091	1.918	4.000	4.000	4.000	1.034	4.000	H2O	1.03	SuM	1.03	0.87	0.87	0.87
Si	1.921	1.921	Si	0.109	0.033	0.000	0.000	0.109	0.114	Si	0.10	Si	0.10	0.19	0.19	0.19	0.19	
Al	0.073	0.073	Al	4.000	4.000	4.000	4.000	4.000	4.000	4.000	Al	1.97	Al	1.97	1.09	1.09	1.09	1.09
ZnO	1.294	1.294	ZnO	3.911	3.917	1.294	4.000	1.294	1.294	1.294	ZnO	100.04	ZnO	100.04	95.89	100.00	100.00	100.00
Cr	0.000	0.140	Fe3+	0.071	0.04*	0.000	0.000	0.071	0.000	0.000	Cr	4.10	Cr	4.10	7.14	7.14	7.14	7.14
Ti	0.00*	Ti	0.015	0.015	0.007	0.007	0.015	0.015	0.015	Ti	1.79	Ti	1.79	0.53	1.10	0.44	0.47	0.47
Fe3+	0.101	ZnO	4.000	4.000	4.000	4.000	4.000	4.000	4.000	Fe3+	0.000	Fe3+	0.000	0.000	0.000	0.000	0.000	0.000
Fe2+	0.227	0.440	Fe2+	3.884	3.823	0.227	2.298	3.820	3.822	3.820	Fe2+	0.755	Fe2+	0.755	0.570	0.430	0.194	1.259
Li	0.003	Li	0.003	0.128	0.128	0.104	0.000	0.003	0.003	0.003	Li	0.027	Li	0.027	0.030	0.008	0.008	0.008
Mg	0.446	0.530	Mg	3.430	3.445	3.220	2.704	3.100	3.242	3.220	Mg	0.013	Mg	0.013	0.033	0.022	0.022	0.022
Cs	0.978	0.340	LiF	0.075	0.173	0.110	0.177	0.220	0.054	0.195	0.140	Fe3+	0.549	Cs	0.111	0.345	0.345	0.345
H2	0.02*	0.140	ZnO	4.044	4.032	4.000	5.941	4.000	4.044	4.071	H2	1.170	H2	1.170	1.192	1.192	1.192	1.192
ZnO	2.004	2.000	ZnO	0.012	0.012	0.000	0.000	0.012	0.012	ZnO	1.047	ZnO	1.047	1.172	1.172	1.172	1.172	
O	4.000	4.000	Gre	0.399	0.399	0.367	0.494	0.294	0.299	0.294	O	13.000	O	13.000	13.000	13.000	13.000	13.000
TiO2	0.00*	TiO2	0.100	0.021	0.015	0.015	0.110	0.011	0.110	TiO2	1.731	TiO2	1.731	1.739	1.920	1.210	1.131	1.131
MgO	0.003	MgO	0.011	0.04*	0.015	0.014	0.014	0.014	0.012	MgO	0.000	MgO	0.000	0.001	0.001	0.001	0.001	0.001
T	0.046	T	0.177	0.125	0.177	0.103	0.145	0.195	0.171	T	0.910	T	0.910	0.790	0.790	0.200	0.343	0.940
Al2O3	0.101	Al2O3	0.101	0.101	0.101	0.101	0.101	0.101	0.101	Al2O3	0.044	Al2O3	0.044	0.013	0.009	0.009	0.009	0.009
Op3	0.047	Op3	0.047	0.047	0.047	0.047	0.047	0.047	0.047	Op3	2.428	Op3	2.428	2.245	2.120	2.043	2.091	2.091
Red	0.197	Red	0.197	0.197	0.197	0.197	0.197	0.197	0.197	OH	2.000	OH	2.000	2.000	2.000	2.000	2.000	2.000
Dm	0.550	Dm	0.550	Chlorite	0.550	0.550	0.550	0.550	0.550	Dm	Proportion of Na+ in lattice sites = 13.43%	Dm	Proportion of Na+ in lattice sites = 13.43%	0.550	0.550	0.550	0.550	0.550
Na	0.253	Na	0.253	Na	0.253	0.253	0.253	0.253	0.253	Na	for Ca, Mg and Fe information of Na+ ambient + negative charges	Na	for Ca, Mg and Fe information of Na+ ambient + negative charges	0.253	0.253	0.253	0.253	0.253
Fe3+	0.305	Fe3+	0.305	Al2O3	17.90	20.00	10.34	20.00	13.33	Fe3+	17.067	Fe3+	17.067	0.90606	0.90606	0.90606	0.90606	0.90606
TiO2	0.07	TiO2	0.07	TiO2	0.07	0.07	0.07	0.07	0.07	TiO2	17.067	TiO2	17.067	0.90606	0.90606	0.90606	0.90606	0.90606
FeO	31.99	FeO	31.99	FeO	31.99	31.99	31.99	31.99	31.99	FeO	30.14	FeO	30.14	37.41	37.41	37.82	37.82	37.82
MgO	11.43	MgO	11.43	MgO	11.43	11.43	11.43	11.43	11.43	MgO	20.18	MgO	20.18	11.90	11.90	13.33	13.33	13.33
LiO	0.33	LiO	0.33	LiO	0.33	0.33	0.33	0.33	0.33	LiO	7.49	LiO	7.49	7.77	7.77	7.77	7.77	7.77
CsO	0.14	CsO	0.14	CsO	0.14	0.04*	0.04*	0.04*	0.04*	CsO	LiO2O3	CsO	LiO2O3	0.07	0.04	0.01	0.01	0.01
H2O	0.07	H2O	0.07	H2O	0.07	0.00	0.00	0.00	0.00	H2O	TiO2	H2O	TiO2	0.11	0.10	0.09	0.09	0.09
H2O	11.13	H2O	11.13	H2O	11.13	11.13	11.13	11.13	11.13	H2O	CaO	H2O	CaO	13.29	13.29	13.45	13.45	13.45
SuM	100.40	SuM	100.40	SuM	100.40	99.27	97.71	97.71	97.71	SuM	H2O	SuM	H2O	1.91	1.87	1.90	1.90	1.90
2	5.473	2	5.473	2	5.473	5.24	5.040	5.24	5.24	2	SuM	2	SuM	99.94	99.94	100.44	100.44	100.44
Al	20.25	Al	20.25	Al	20.25	20.47	20.47	20.47	20.47	Al	2	Al	2	3.000	3.000	3.000	3.000	3.000
Al	2.203	Al	2.203	Al	2.203	2.457	2.457	2.457	2.457	Al	2	Al	2	2.411	2.411	2.400	2.400	2.400
Ti	0.012	Ti	0.012	Ti	0.012	0.003	0.003	0.003	0.003	Ti	0	Ti	0	0.004	0.004	0.004	0.004	0.004
Li	0.044	Li	0.044	Li	0.044	0.042	0.042	0.042	0.042	Li	0	Li	0	0.003	0.003	0.001	0.001	0.001
Fe	5.743	Fe	5.743	Fe	5.743	5.120	5.740	5.120	5.120	Fe	0	Fe	0	0.420	0.420	0.400	0.400	0.400
LiF	3.979	LiF	3.979	LiF	3.979	4.022	4.230	4.022	4.022	LiF	0	LiF	0	3.074	3.074	3.022	3.022	3.022
Ca	12.000	Ca	12.000	Ca	12.000	11.891	12.000	11.899	11.899	Ca	0	Ca	0	2.003	2.003	2.001	2.001	2.001
H2	0.038	H2	0.038	H2	0.038	0.000	0.000	0.000	0.000	H2	0	H2	0	2.001	2.001	2.000	2.000	2.000
Cs	0.034	Cs	0.034	Cs	0.034	0.014	0.014	0.014	0.014	Cs	0	Cs	0	1.000	1.000	1.000	1.000	1.000
OH	14.000	OH	14.000	OH	14.000	14.000	14.000	14.000	14.000	OH	0	OH	0	12.122	12.122	12.127	12.127	12.127